1st Croatian Conference on Earthquake Engineering
1CroCEE
22-24 March 2021 Zagreb, Croatia

DOI: https://doi.org/10.5592/CO/1CroCEE.2021.27

Performance of a Brb RC high-rise building under successive application of wind-earthquake scenarios

Ahmad Naqi[1], Taiki Saito[2]

[1] *Graduate Student*, Department of Architecture & Civil Engineering, Toyohashi University of Technology, *ahmad.naqi.sl@tut.jp*

[2] *Professor*, Department of Architecture & Civil Engineering, Toyohashi University of Technology, *tsaito@ace.tut.ac.jp*

Abstract

High-rise buildings in the regions with multi-hazard (MH) events, such as wind and earthquake, are exposed to more than one type of lateral excitations which act in consecutive manner. Conventionally, in such regions, the maximum of each MH event is used separately to evaluate the performance of buildings while the contribution of preceding event is neglected. When using vibration control devices such as steel dampers, which are effective against both earthquake and wind, accumulation of damage due to continuous input may become a problem. Thus, the current research work aims to investigate the contribution of preceding MH event to the performance of buildings. In this regard, a 20-story RC frame with supplemented buckling-restrained brace (BRB) is designed to satisfy the criteria under the Level-2 earthquake ground motions recommended in Japanese design standard. Then, a total of 16 sets of MH scenarios are created by combining four sets of preceding wind loads with different intensities (17, 20, 25 & 31 m/s of mean speed) and four sets of succeeding earthquake loads of Level-2 intensity. The performance of the RC frame is evaluated in terms of global parameters (such as, natural periods, mode shapes, inter-story drifts, roof displacement profiles, and residual displacements) and BRBs parameters (such as, ductility demands, cumulative plastic deformations, and force-deformation relations). It is observed that the performance of the building with BRB is significantly affected under the successive application of wind-earthquake scenarios in comparison to the application of the single hazard. This result suggests the importance of considering multi-hazard events in the design of buildings.

Key words: buckling-restrain brace, RC high-rise building, earthquake, wind, multi-hazard, successive analysis

1 Introduction

For earthquake and wind loads, most of worldwide building codes consider the single hazard (SH) for the structural design, and do not consider the successive events because of its low occurrence probability and cumbersome calculation [1]. However, when hysteresis dampers such as buckling-restrained braces (BRBs) are used as vibration control devices for high-rise buildings, fatigue due to the accumulation of plastic energy against successive events cannot be ignored. Therefore, multi hazard (MH) scenarios involving winds and earthquake ground motions are considered in this study, and the structural performance of a 20-story RC building enhanced with BRBs is examined to clarify the effect of the sequence of hazards to the damage of both the building and the BRB devices.

2 Prototype RC frame enhanced with BRBs

A 20-story RC moment resisting frame is designed to resist the gravitational loads and then the BRB devices are selected to minimize the inter story drift ratio below 1 % under lateral excitation of Level-2 earthquakes [3]. It is assumed that the prototype building is located in Aichi Prefecture, Japan. As presented in Fig. 1a, the prototype building is a plane frame consisting of 5-span with a total length of 27.2 m and the story height is 4.5 m on the first floor and 4 m on the other floors. Structural parameters of the RC columns and beams are summarized in Table 1. The prototype building is enhanced in each floor by two diagonal BRBs installed symmetrically. The parameters of BRB devices are summarized in Table 2.

Earthquake response of the frame model is calculated by STERA_3D (STructural Earthquake Response Analysis 3D) software, which is a finite element-based software developed by one of the authors [5]. In the software, the beam elements are presented by two nonlinear flexural springs at both ends and one shear spring at the middle. The column elements have nonlinear axial springs distributed in the sections of both ends and two nonlinear shear springs in the middle to represent the directional properties of the element. The hysteresis model of nonlinear bending springs for column and beam elements is the degrading trilinear model as shown in Fig. 1b. The beam-column connection is assumed rigid, where the rigid zone length for beam element is set to be half of the column width. For both beam and columns, the steel strength is modified 1.1 times than the nominal strength and the ratio of post-yield stiffness is $\gamma = K_0/K_y = 0.001$. The BRB element is defined as a shear spring in a frame with the bi-linear hysteresis with initial stiffness, K_1, and secondary stiffness of, K_2, as shown in Fig. 1c. The wind loads in STERA-3D are applied at the centre of gravity at each floor, while the load distribution factor according to the Japanese standard is used to distribute the load along the height.

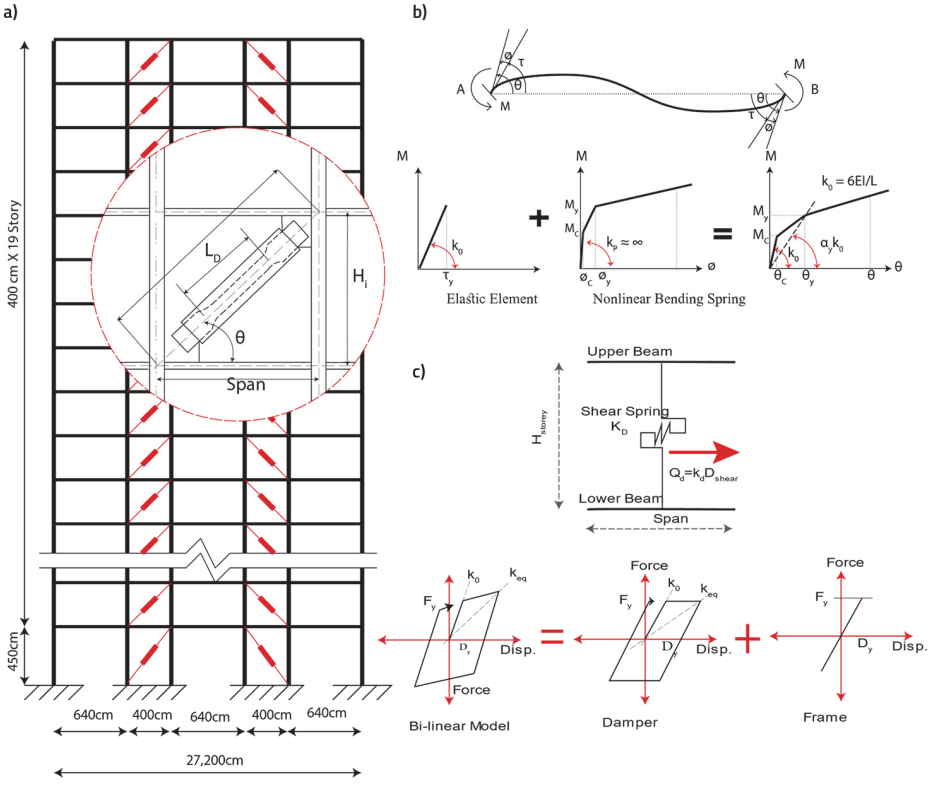

Figure 1. a) The prototype building elevation and BRB configuration; b) Hysteresis model of nonlinear bending spring of beam and column elements; c) Bi-linear hysteresis model of nonlinear shear spring for BRBs.

Table 1. Structural parameters of RC columns and beams in prototype Building

Story	Column			Story	Beam			
	Fc [MPa]	D×B [cm]	Main Reinforcement		Fc [MPa]	D×B [cm]	Main Reinforcement	
							Top	Bottom
18-20	32	50×50	16-D19	16-20	32	60×50	5-D20	5-D20
13-17	36	55×55	16-D20	11-15	36	60×50	5-D22	5-D22
8-12	42	60×60	16-D22	6-10	42	65×55	5-D22	5-D22
4-7	48	65×65	16-D22	2-5	42	65×55	5-D22	5-D22
1-3	52	70×70	16-D25	1	48	65×60	4-D25	4-D25
	1) For the entire beams and columns, the shear reinforcement is D13@100 mm. 2) For both column and beams the tensile strength of main & shear reinforcement are 490 MPa & 295 MPa, respectively.							

Table 2. Structural parameters of BRB members

Story	Story weight [kN]	Story height [cm]	K_0 [kN/mm]	F_y [kN]	K_1/K_0
20	2275.0	400	80	520	0.02
18-19	2082.5	400	80	520	0.02
14-17	2082.5	400	100	650	0.02
11-13	2082.5	400	120	780	0.02
8-10	2082.5	400	130	845	0.02
5-7	2082.5	400	120	780	0.02
2-4	2082.5	400	110	715	0.02
1	2187.5	450	80	520	0.02

3 Multi-hazard scenarios (MH)

During the lifetime of a building, the possibility of earthquake events preceded by wind events, or vis versa, is significantly high in the area like Japan which is prone to earthquakes and typhoons [4]. The objective of the current study is to evaluate the performance of the target building under different scenarios of successive wind and earthquake loadings. Fig. 2 shows two different scenarios; one is the wind comes first followed by the earthquake (wind-earthquake), and the other is the order is reversed (earthquake-wind). Four sets of earthquake ground motions are combined with four sets of winds of different intensities. Table 3 presents the detail of four selected earthquakes. The earthquakes are consisting of two observed earthquake ground motions scaled to match the maximum velocity of 50 cm/sec [6] and two ground motions artificially generated from the phase spectrum of historical earthquakes to be compatible with the extreme rare earthquake (Level-2) acceleration response spectrum defined by Building Standard Law of Japan [3]. In case of wind events, four sets of wind excitation are generated according to the Architectural Institute of Japan (AIJ) 2019 recommendation [2], namely; the weak winds (17 m/sec of frequent occurrence), moderate winds (20 m/sec of 1-year return period), rare wind (25 m/sec of 10-years return period), and extremely rare wind (31 m/sec of 50-years return period). For each of the four wind intensities, 10-minutes fluctuating component of wind time-history profile is generated using the von Karman spectrum which is recommended in AIJ 2019 [2].

Table 3. List of selected earthquake ground motions

No.	Categories	Event	Date	Station	Abbreviation
1	Scaled earthquake to be compatible of 50 (cm/sec)	Imperial Valley	1940	El Centro	ELC
2		Kern County	1952	Taft	TAF
3	Artificially generated earthquake to be compatible of L2	Tokachi Oki	1968	Hachinohe	HAC
4		Kobe	1995	JMA	KOB

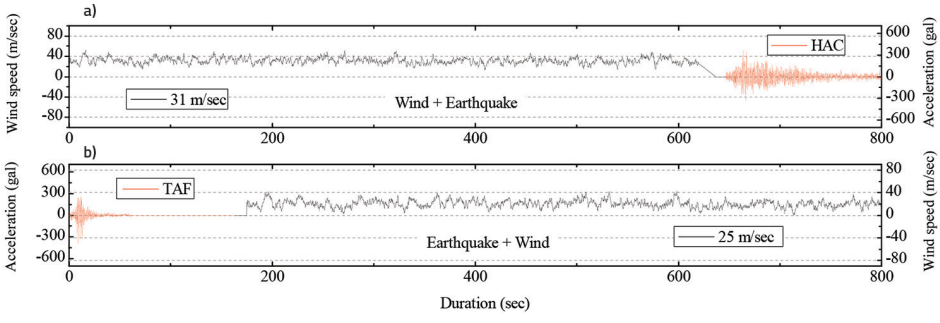

Figure 2. Multi-hazard scenarios, a) wind-earthquake (W31-HAC); b) earthquake-wind (TAF-W25).

4 Results of successive analysis of prototype building

4.1 Natural period of the building

The difference of the natural period of the building between pre- and post-earthquake or wind excitation due to the damage and stiffness degradation of structural members is examined [7]. As presented by the dotted line in Fig. 3, the natural periods of 1st, 2nd, and 3rd modes under the free vibration (pre-event) are 2.379, 0.797, and 0.430 sec, respectively. As presented by the event number 1, 2, 3, and 4 in Fig. 3, the natural periods after application of four earthquakes are 3.588~3.704 sec for the 1st mode, 1.107~1.119 sec for the 2nd mode, and 0.527~0.558 sec for the 3rd mode of vibration which indicates the natural period is elongated about 50~55 % for the 1st mode, 38~40 % for the 2nd mode, and 28~30 % for 3rd mode, respectively. Similarly, as presented by the event number 5, 6, 7, and 8 after individual application of wind events, it is observed the natural period is elongated 2.621~ 3.377 sec for the 1st mode, 0.842 ~1.027 sec for the 2nd mode, and 0.45 ~0.52 sec for the 3rd mode, respectively. There is a noticeable difference in the natural period due to the wind intensity.

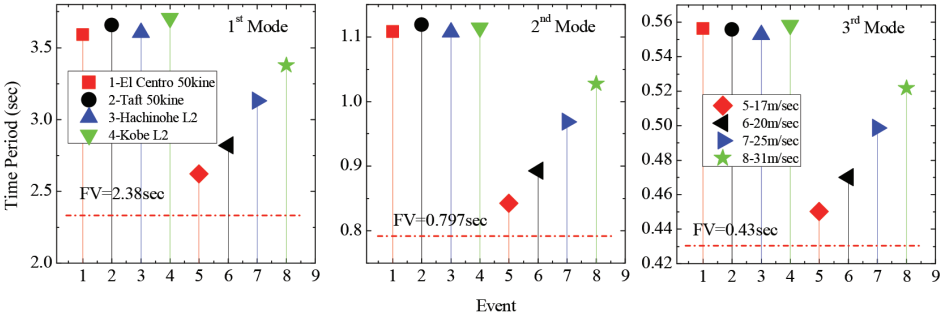

Figure 3. Comparison of natural periods between pre-event (FV) and post-event of earthquake or wind

The post-event natural periods of MH scenarios are compared with the free vibration and SH as well. Fig. 4 shows the 1st mode natural periods of SH of earthquake and MH of wind-earthquake. It can be seen that the difference of natural periods between SH are MH is small. Fig. 5 shows the 1st mode natural periods of SH of wind and MH of earthquake-wind. Although the post-event natural period of SH increases in wind intensity, it doesn't affect the natural period of MH. This means that the effect of wind is small with respect to the change of the natural period.

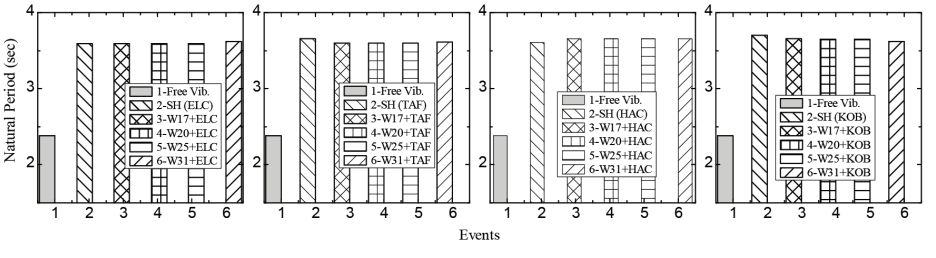

Figure 4. Comparison of the natural period between SH (earthquake) and MH (wind-earthquake)

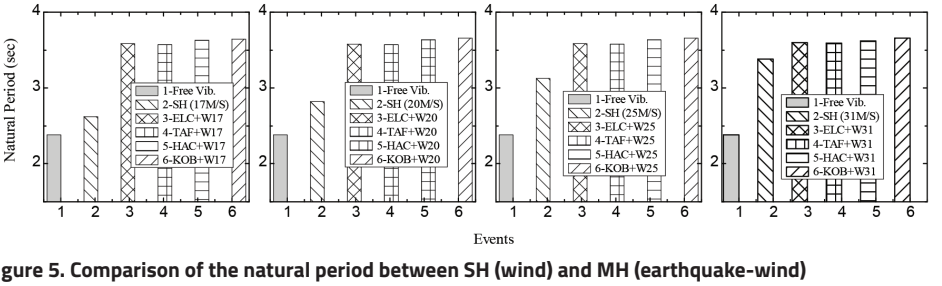

Figure 5. Comparison of the natural period between SH (wind) and MH (earthquake-wind)

4.2 Maximum story drift of the building

The maximum inter-story drift ratios, which are obtained from the time history analyses of SH and MH, are compared. Fig. 6 shows the maximum story drift ratios of SH of earthquake and MH of wind-earthquake. It is interesting to note that when the wind precedes the earthquake, the subsequent earthquake does not necessarily increase the response, but may even decrease it. It is assumed that the change of natural period after wind event affects the subsequent earthquake response.

Fig. 7 shows the maximum story drift ratios of SH of wind and MH of earthquake-wind. When the earthquake precedes the wind, the change in the maximum response due to the subsequent earthquake is large. It increases in the order of KOB, ELC, HAC, and TAF.

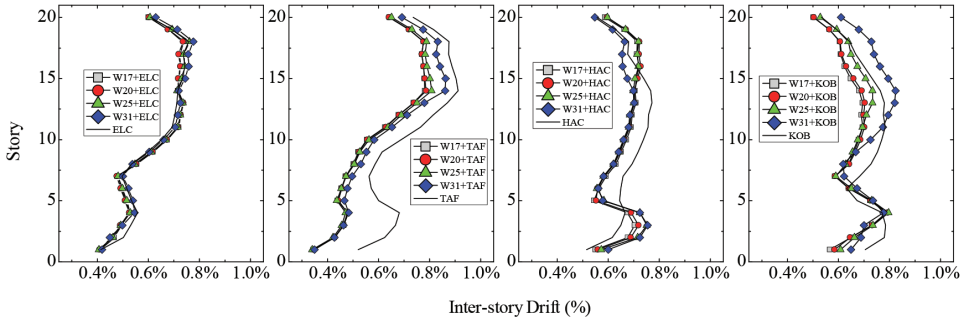

Figure 6. Comparison of the maximum story drift ratio between SH (earthquake) and MH (wind-earthquake)

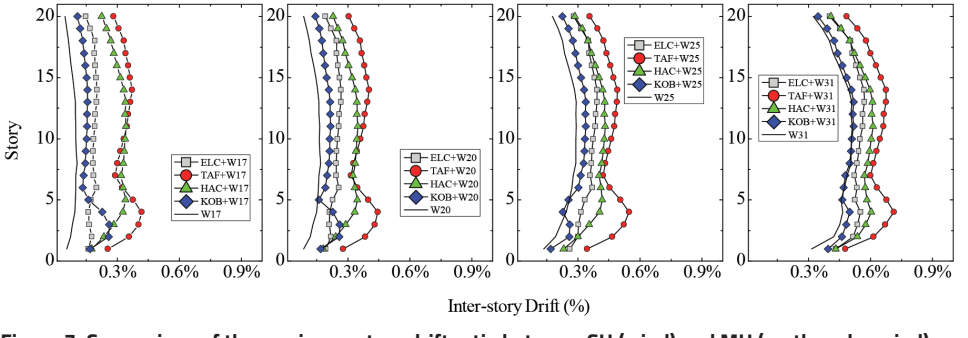

Figure 7. Comparison of the maximum story drift ratio between SH (wind) and MH (earthquake-wind)

4.3 Roof displacement profile

Fig. 8 compares the maximum roof deformation between SH and MH. It is seen from Fig. 8a, the maximum roof displacement of SH (earthquake) is larger than MH (wind-earthquake) except ELC. In case of MH of earthquake-wind, as shown in From Fig. 8b, the maximum roof displacements increase with wind intensity. The same trend can be seen for the residual deformation as presented in Fig. 9.

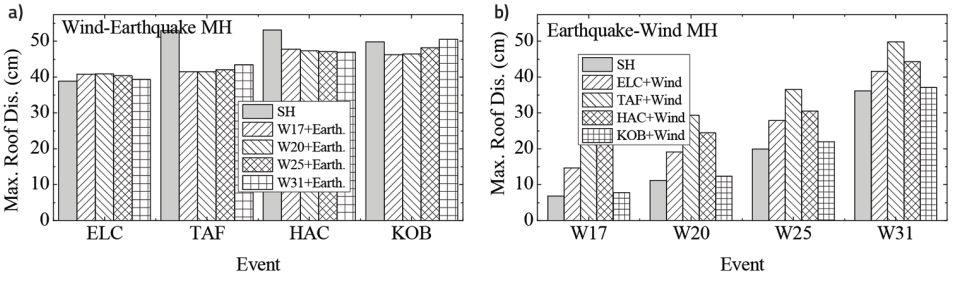

Figure 8. Comparison of the maximum roof displacement between SH and MH, a) SH (earthquake) and MH (wind-earthquake), b) SH (wind) and MH (earthquake-wind).

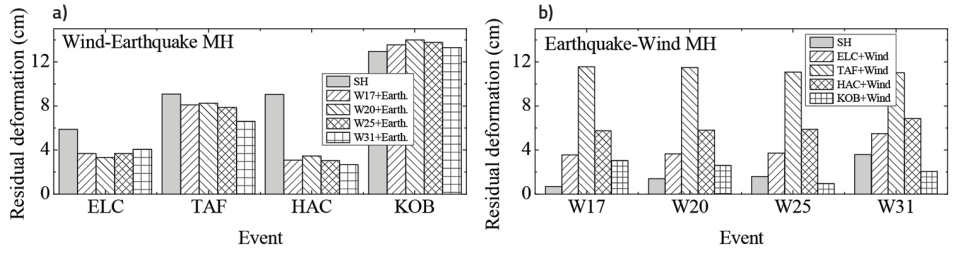

Figure 9. Comparison of the residual deformation between SH and MH, a) SH (earthquake) and MH (wind-earthquake), b) SH (wind) and MH (earthquake-wind)

4.4 Energy absorption rate

Fig. 10 shows the amount of hysteresis energy absorbed by load-resisting members (columns, beams, and dampers) of the building under the SH and MH events. From Fig. 10a, the cumulative energy dissipation of MH (wind-earthquake) increases in comparison to SH (earthquake) by ~3 %, ~7 %, ~50 %, and ~149 % corresponding to the preceding wind loads of 17, 20, 25 and 31m/sec. Similar trend is observed for MH (earthquake-wind) scenarios as well as shown in Fig. 10b.

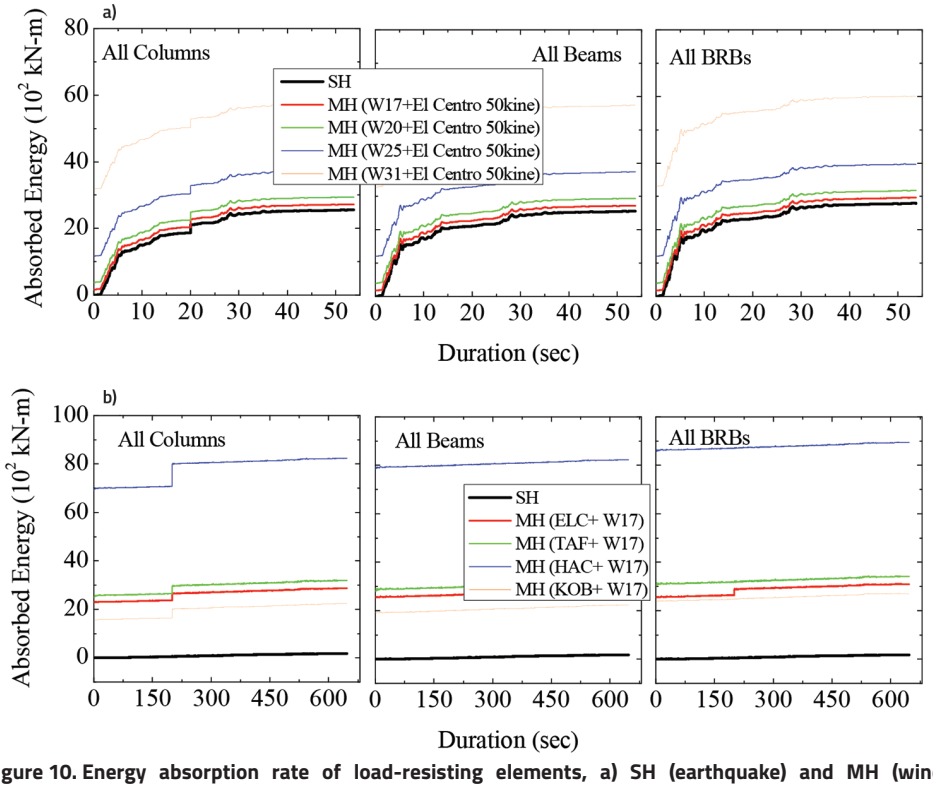

Figure 10. Energy absorption rate of load-resisting elements, a) SH (earthquake) and MH (wind-earthquake), b) SH (wind) and MH (earthquake-wind).

4.5 Cumulative ductility factor and plastic strain energy of BRBs

The accumulative damage of BRBs is evaluated in the term of the cumulative ductility factor (CDF) and the plastic strain energy (PSE) [8]. As presented in Fig. 11, the plastic strain energy is defined as the ratio of area of plastic strain energy by the triangular area shaped by the yield and deformation strengths of RBR. The cumulative ductility factor is the normalized summation of total plastic deformation to the yield deformation of BRB.

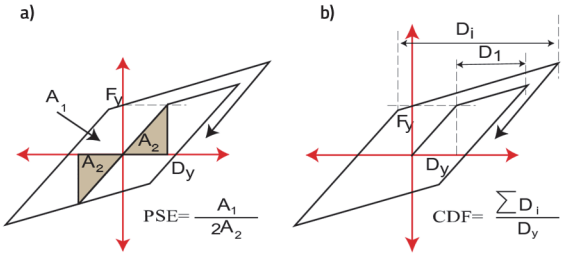

Figure 11. a) Plastic Strain Energy (PSE), b) Cumulative Ductility Factor (CDF).

Fig. 12 presents the force-deformation (strain) relationship of the BRB installed in the first floor of the building. From Fig. 12a, under successive analysis of MH (wind-earthquake), the shape of the force-deformation relationship is different from SH (earthquake), and PSE and CDF are increased about 1~5 % and 50~300 % corresponding to the preceding wind intensity. As shown in Fig.12b, the value of PSE for SH (wind of 31m/sec) is small at 0.02, while the value of CDF is large at 20.54. This is related to the long duration of the wind.

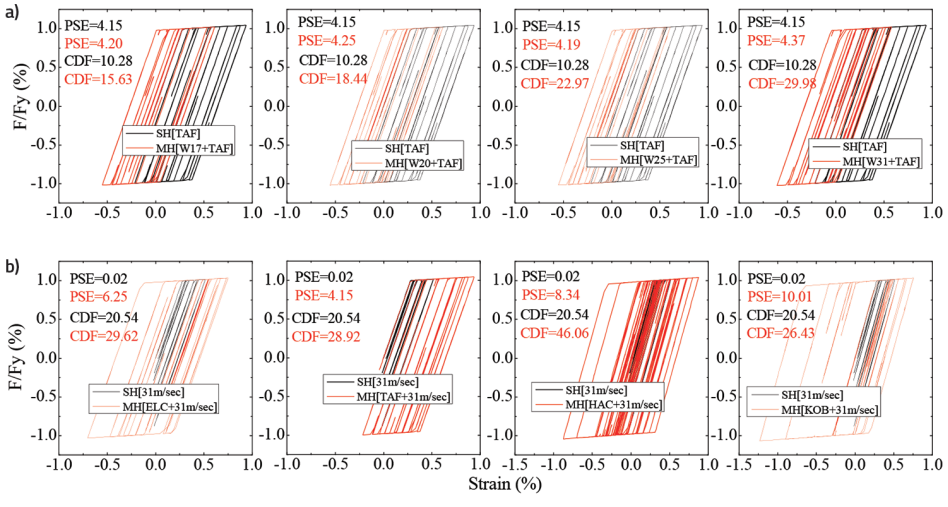

Figure 12. Force-deformation relationship of BRBs, a) SH (earthquake) and MH (wind-earthquake), b) SH (wind) and MH (earthquake-wind).

5 Conclusion

The performance of the high-rise RC building with BRB dampers is investigated under successive application of MH scenarios of earthquakes and winds. It is observed, although the effect of wind load is small with respect to the overall performance of prototype building, its effect to the cumulative ductility factor and plastic strain energy of BRBs cannot be neglected.

References

[1] Duthinh, D., Simiu, E. (2010): Safety of structures in strong winds and earthquakes: Multihazard considerations. *Journal of Structural Engineering*, **136** (3), 330-333, doi: https://doi.org/10.1061/(ASCE)ST.1943-541X.0000108

[2] AIJ (2019): Recommendations for loads on buildings, Architectural Institute of Japan.

[3] Building Standard Law of Japan (2004): The building Centre of Japan.

[4] Roy, T., Saito, T., Matsagar, V. (2021): Multi-hazard framework for investigating high-rise base-isolated buildings under earthquakes and long duration winds. *Earthquake Engineering and Structural Dynamics*, 1-24, https://doi.org/10.1002/eqe.3401

[5] Saito, T. (2019a): STructural Earthquake Response Analysis 3D version 10.3 (STERA_3D v10.3), http://www.rc.ace.tut.ac.jp/saito/software-e.html (accessed on Wednesday, 13 January 2021).

[6] Saito, T. (2019b): STructural Earthquake Response Analysis WAVE version 1.0 (STERA_WAVE v1.0), http://www.rc.ace.tut.ac.jp/saito/software-e.html (accessed on Wednesday, 13 January 2021).

[7] Vidal, F., Navarro, M., Aranda, C., Enomoto, T. (2014): Changes in dynamic characteristics of Lorca RC buildings from pre- and post-earthquake ambient vibration data. *Bull Earthquake Engineering,* **12**, 2095–2110. https://doi.org/10.1007/s10518-013-9489-5

[8] Iwata, M., Murai, M., (2006): Buckling-restrained brace using steel mortar planks; performance evaluation as a hysteretic damper. *Earthquake Engineering Structure Dynamic*, **35** (14), 1807-1826. https://doi.org/10.1002/eqe.608